A computer-vision based precision seed drill guidance assistance

V. Leemans, M.-F. Destain

Gembloux Agricultural University, Unité de Mécanique et Construction, Passage des Déportés 2, B 5030 Gembloux, Belgium

Abstract: This paper presents a control mechanism aiming to position seed drills relative to the previous lines, while sowing. The position was measured by a machine vision system and used in a feedback control loop. An articulated mechanism was used to ensure the lateral displacement of the drill relative to the tractor. The behaviour of the whole outfit was studied during several field tests. The standard deviation of the error, measured as the difference between the observed inter-row distance and its set value, was 23 mm and its range was less than 100 mm, which was sufficient to fulfil the requirements of the application. Sources of systematic errors were also identified as linked to the geometric considerations. Their correction requires an accurate mounting of the camera, which may be possible for a serial montage.

Keywords: Automatic guidance; Seed drill; Hough transform; Machine vision

1. Introduction

The lateral position of a seed drill relative to a previous passage is usually controlled by the driver of the tractor. The accuracy of this task determines the feasibility and performance of subsequent works like mechanical weeding or harvesting with machines having a width not matching the seeding width (in term of line number). For example, most sugarbeet seed drills in Belgium are of 12 rows width while the harvesters are of 6 rows. Some machine manufacturers, however, have shown an interest in eight-row-harvesters to enhance the harvesting performances. To operate a harvester of one configuration on a field sown using a different configuration, the range of the movements of the drill needs to be kept to less than 150 mm around the nominal inter-row spacing (usually 450 mm for sugarbeet). Though an experienced operator may be able to achieve the required driving performance, this task requires concentration and is difficult to maintain for a long period of time. The supervision of the drill itself is also part of the driver's task and adds to the driver's load. Under these circumstances, driving assistance would be welcome.

The problem of automatically guiding a tool in a field using machine vision is not new. This literature review is limited to papers concerning prototypes used for field agricultural applications. Recent researches can be divided into either autonomous steering or guidance assistance. The techniques were used to evaluate the position of the tool in the field relative to the crop rows or to the edge of the harvested part of the field. For each research, the hardware is presented first, the image analysis techniques are described and finally the post-processing of the rough data extracted from the image (and from other sensor, if applicable), used to control the actuator are mentioned.

Billingsley and Schoenfisch (1997) presented a method to steer a tractor by following crop rows such as cotton. For this kind of crop, depending on the stage of growth, the row does not always appear continuous in the images. In order to localise crop rows, the pixels were segmented between 'plant' and the surrounding by thresholding, the value of the threshold being determined by the proportion of the image occupied by plants. The row detection algorithm searched lines by regression, in 'viewports' centred on the previous detected rows. The fitted lines were defined by an offset and a slope parameters, in direct relation with the state variable of the vehicle location (the lateral position of the tractor, the heading angle and the steering angle).

Hague et al. (2000) presented an experimental autonomous vehicle guided by a machine vision system and additional sensors (odometers and inertial sensors). This vehicle was able to follow cauliflowers rows and to ensure a dead reckoning. A Hough transform was used to localise the row structure and an extended Kalman filter ensured the fusion of the different sensors information and to obtain the position of the vehicle.

Tillett and Hague (1999) and Tillett et al. (2002) developed a hoeing system for weed control in sugar beets. The camera was mounted on a hoe attached to the tractor three-point linkage through a mechanism allowing a lateral displacement. The camera was a mono-chrome charge-coupled device (CCD) equipped with a near infra-red

bandpass Alter. Its height was of 1.14 m and inclined at 40° on the vertical. The lateral displacements were controlled by two hydraulic cylinders and the hydraulic flow was commanded by a three-position-valve. A linear variable differential transformer gave the lateral position of the hoe. In Tillett et al. (2002), the image was divided horizontally into height bands. Each of these sub-images were merged vertically to give horizontal profiles. The position of the crop rows were found by matching a template profile. The extended Kalman filter was used to track the lateral position of the hoe relative to the rows. The measurements were made up of the position in each band and the state vector had three elements: the lateral position, the heading angle and a correction for the camera misalignment. During the computation of the recursive Alter, the error between the measured and the expected position was evaluated. If this value was too big, the data were ignored, otherwise they were incorporated in the state estimation. The trueness was below 10 mm, while the precision was within 16 mm. Authors also presented the minimum development stage required and the behaviour in presence off gaps in the culture rows.

Pilarski et al. (2002) presented an automated self-propelled windrower with a control based on a camera or on a differential global positioning system (DGPS) associated with other sensors (inertial and wheel encoder). These systems were tested independently to harvest a field autonomously, after the 'opening up' by a human operator. Two cameras were mounted on the side of the cab of a self-propelled windrower. The edges of the cut and uncut areas were localised using the difference in reflectance, after a compensation of the shadows. Authors also detected the end of crop row (where there was no more edge) and obstacles (based on their different colour). The DGPS data were acquired at 5 Hz and other sensors were used to extrapolate the position. The system could work at 1.5-2.0 m/s. The vision-based error was in range of 50-300 mm, while the error of the DGPS was in a range from 40 to 60 mm.

Søgaard and Olsen (2003) mounted a camera on a hand-operated vehicle and later on a weeder to evaluate the precision of an algorithm based on image analysis. The camera height was of 1.15 m and the inclination of the optical axis on the vertical of 56°. The images were also divided into band strip, which were mathematically 'enrolled'. The centre of gravity gave the position and an estimation of the relative accuracy. A weighted linear regression gave the position of the rows. The mean position returned by their algorithm (trueness) was centred with the reference trace, with no statistical differences. The standard deviation (precision) was below 5 mm in the centre of the image and about three times higher under the camera (this was 1.73 m at the rear of the image centre). The working speed was of 0.4 m/s. These results, however, concerned the image analysis, not the position of a tool.

The aim of this work was similar to row tracking, but there is a significant difference: the detection was based on images where, being of the same nature, there was poor contrast between a target (the seed lines) and its surrounding. In a previous paper (Leemans and Destain, 2006), a background subtraction and a modified Hough transform were used to localise the seed lines. The noise was neither Gaussian nor white. In those circumstances, a non-linear recursive Alter gave better results than the Kalman Alter. This paper aims to show that the signals issued from that process are useful to control the lateral seed drill movements.

2. Materials and methods

2.1. The hardware

The field experiments were carried out using a precision seed drill ("Précis +", six rows, Gilles S.A., Belgium) coupled to a tractor via a lateral positioning device, as shown in Fig. 1. The lateral positioning device was a piece of a mechanically guided hoe (from Agronomic, France) composed of two frames, attached, respectively, to the tractor and to the tool and joined by two links. The lateral movements were produced by two cylinders, controlled by a three-way 'right on-off - left on - valve', itself driven by a laptop computer, using its parallel interface. A joystick could also be used by the operator for manual control. Preliminary tests showed that the engine speed had a limited impact on the lateral speed of the seed drill relatively to the tractor (the lateral speed grew by 25% when the engine speed doubled).

The relative lateral position of the seed drill compared to the previous lines was recorded by a camera fixed to the drill (Fig. 1, unless otherwise stated, 'position' will hereafter always refer to the lateral position of the drill relative to the previous rows). The camera was placed offset, above the two previous seedbed lines, at a height of 0.7 m and its optical axis was 65° with the vertical. This allowed the two lines to be visible in the image. The camera was a Unibrain Fire-iA400 1394 colour mono-CCD (Unibrain S.A., Greece) equipped with a 6 mm focal length lens. The automatic settings of the electronic shutter were found suitable for the application. The camera was controlled by the computer through the IEEE 1394 port via a '1394 Digital Camera Driver' (The Robotic

Institute, Carnegie Mellon University, PA, USA).

Fig. 1. *Experimental set up used for the field tests. The seed drill was coupled to a frame allowing lateral movements relative to the tractor. The camera was used to record the position of the drill relatively to the previous seed lines.*
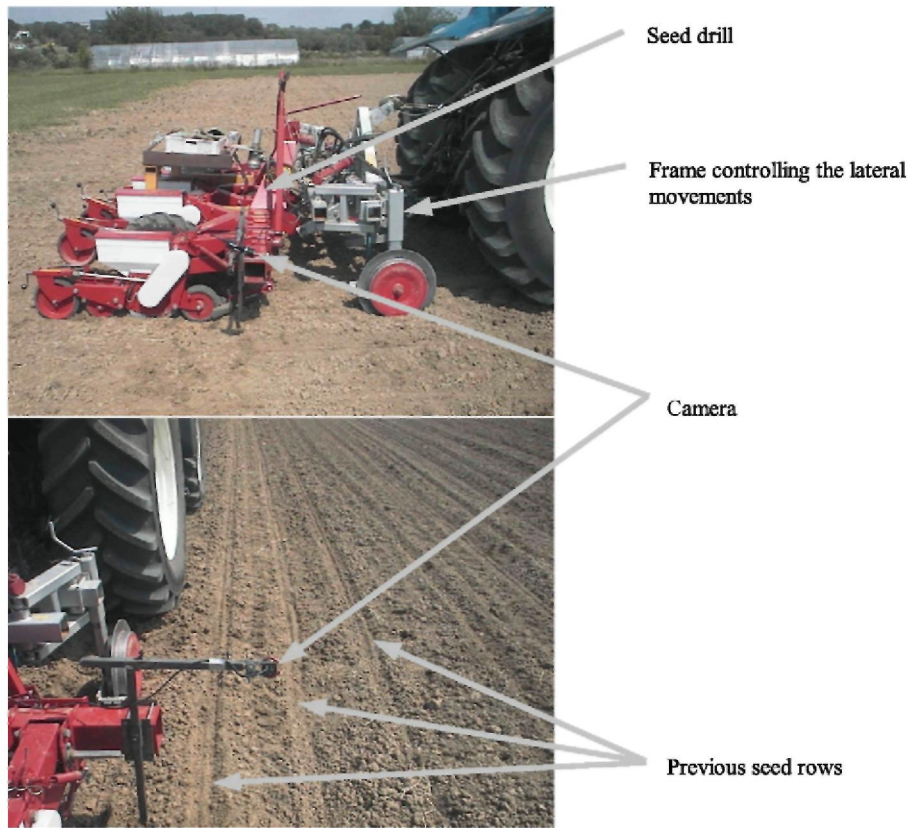

Fig. 2. *The feedback loop used in the proposed regulation. The 'target position' is the lateral position that the right seed line should occupy, at the bottom of the image, provided that the seed drill is correctly positioned, Δx is the error, in mm; At is the time in ms that the actuator should work to compensate Δx; r_m is the measured distance between the actual row and the nominal one, perpendicularly to this later, in pixels; θ_m is the measured angle of the actual row and the nominal one, in radians (both r_m and θ_m are measured in the image plane); $\hat{\theta}$ and $\hat{r}$ are the corresponding estimated parameters; $\hat{x}_b$, is the estimated position of the right line at the bottom of the image.*
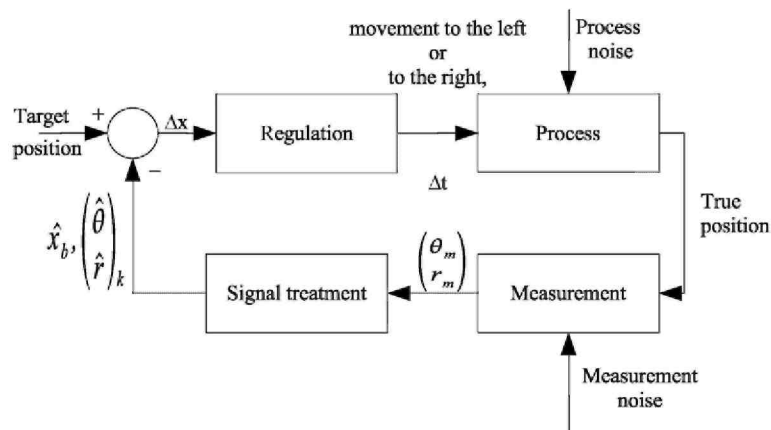
2.2. The algorithms

The control of the position of the seed drill corresponds to the general block diagram presented in Fig. 2. The

true position was evaluated by using image acquisition, treatment and analysis (the measurement). This process suffered from measurement noise and the signal calculated through image analysis was therefore treated before being used. The estimated position was then compared with the reference. The error Δx was transformed into a pulse driving the opening of the valve, the pulse width was related to the value of Δx with the sign of the error determining the direction of the movement. The translation device converted it into a lateral displacement of the seed drill (process). The new position resulted from the addition of this displacement and of the lateral and angular movements from the tractor (the process noise) to the previous position.

2.2.1. The measurement

The camera output was 640 × 480 pixels RGB colour images, with a 15 Hz update rate.

The integration time, the brightness and the gain were adjusted automatically by the camera. The green channel was used and the image size was reduced to 106 × 80 pixels, to reduce the computational load.

The base of the image treatment were described in Leemans and Destain (2006). The sowing lines appeared as dark thin lines on a brighter background, but the 'noise' was important relative to the relevant information. The image treatment consisted in a Gaussian filtering (3x11 pixels-the basic image treatments were carried out using the 'Open Source Computer Vision Library', Intel Corporation, CA, USA) and a background compensation to remove the shadows. The background was computed using a wide median filter (5 × 5pixels), which preserved the boundaries of the wide objects present in the image while removing the narrow linear elements. Subtracting the image from the background gave an image with the sowing lines appearing as bright lines on a dark surrounding. The detection was performed using a modified Hough transform. The basic idea was to perform one transform for each line with a specific reference point corresponding to each line in the cluster. The result of this treatment were the Hough space coordinates of the rows relative to the reference rows (the row when the drill is parallel to the previous rows and at the set distance of 450 mm to the previous row). The first coordinates was the measured distance r_{m} between the actual rows and their set position, perpendicularly to these later and at mid height of the image.

The second coordinate was the measured angle θ_{m} of the actual rows and the reference rows. Both r_{m} and θ_{m} are measured in the image plane, and are the same for each row.

2.2.2. The signal treatment

The position of the seed drill was evaluated using the lateral position of the right line at the bottom of the image ($\hat{x}_{\mathrm{b}}$) given by:

$$\hat{x}_{\mathrm{b}} = x_{\mathrm{r}} + \frac{\hat{r}}{\cos(\hat{\theta} + \theta_{\mathrm{t}})} + \frac{h}{2}\tan(\hat{\theta} + \theta_{\mathrm{t}}) \tag{1}$$

where x_{r} is the theoretical position of the right line at mid-height of the image; $\hat{\theta}$ and $\hat{r}$ are the estimated Hough space coordinates; θ_{T} is the theoretical angle between the right line and the vertical in the image; h is the image height. All the linear parameters were measured in pixels and the angles in radians, $\hat{x}_{\mathrm{b}}$ is converted into mm before being recorded, using the image scale at the bottom of the image (1.1 pixels/mm), in order to be compared to the ground measurements. The estimated Hough space coordinates $\hat{\theta}$ and $\hat{r}$ were used as state variables. These parameters were estimated independently (at step k), using a non-linear recursive filter combining their measures in the image θ_{m} and r_{m}, their previous estimations (at step k-l) and the shift caused by the control Δr_{r}:

$$\begin{pmatrix} \hat{\theta} \\ \hat{r} \end{pmatrix}_{k} = \begin{pmatrix} a_{\theta} & 0 \\ 0 & a_{\mathrm{r}} \end{pmatrix} \begin{pmatrix} \theta_{\mathrm{m}} \\ r_{\mathrm{m}} \end{pmatrix}_{k} + \begin{pmatrix} 1 - a_{\theta} & 0 \\ 0 & 1 - a_{\mathrm{r}} \end{pmatrix} \begin{pmatrix} \hat{\theta} \\ \hat{r} \end{pmatrix} + \begin{pmatrix} 0 \\ \Delta r_{\mathrm{r}} \end{pmatrix}_{k-1} \tag{2}$$

$$a_{\theta} = c_{\theta} \exp\left(\frac{-[(\hat{\theta})_{k-1} - \theta_{\mathrm{m}}]^2}{s_{\theta}^2} \right) \tag{3}$$

$$a_{\mathrm{r}} = c_{\mathrm{r}} \exp\left(\frac{-[(\hat{r} + \Delta r_{\mathrm{r}})_{k-1} - r_{\mathrm{m}}]^2}{s_{\mathrm{r}}^2} \right) \tag{4}$$

where c_{θ}, s^2_{θ}, c_{r} and s_{r}^2 are parameters adjusted empirically on measurement made on videos acquired in field (Leemans and Destain, 2006). When the measurement was close to the previous estimation, a_{θ} or a_{r} were near their respective maximal values of c_{θ} or c_{r}. Otherwise, the value of a_{θ} or a_{r} decreased and the weight of the measurement decreased accordingly. The earlier version of the algorithm used to process these videos showed

that the measurement noise was not Gaussian but included multiple type of noises and this non-linear recursive filter was then found useful.

When the seed drill is not parallel to the previous rows, i.e. when θ was different from 0, the seed drill has a lateral movement and the true value of r_m change from one image to the other. This effect could be estimated and incorporated in Eq. (2) and laboratory tests showed that taking into account the angle between the seed drill and the rows enhance the estimation of the position. However, this required an accurate camera alignment, which was difficult to achieve in the field (the main problem was to ensure that the drill was quite perpendicular to the previous lines-because the camera was removed during transports, it could not be done in the laboratory) and was thus not used for the field tests.

The lateral movement of the seed drill would also result in a change in the apparent angle of the row in the trace. However, as the lateral displacements were limited by the control itself, this was not considered.

2.2.3. The control and the process

The lateral displacement of the tool relative to the tractor was controlled by adjusting the pulse width signal sent to the valve, which controlled the opening of the valve. The relation between the pulse width and the lateral displacement was analysed and between 20 and 200 ms, a linear relationship between the lateral speed υ (mm/ms) and the pulse width Δt (ms) was found. Below 20 ms, the valve did not open and above 200 ms (which is far more than the interval between two images), the speed did not depend on the pulse width. The opening time for a given error Δx (mm) was thus given by:

$$v = p\Delta t + q \tag{5}$$

$$v = \frac{\Delta x}{\Delta t} \tag{6}$$

By eliminating υ between Eqs. (5) and (6), it comes

$$p\Delta t^2 + q\Delta t - \Delta x = 0 \tag{7}$$

$$\frac{\Delta t'}{\Delta t''} = \frac{-q \pm \sqrt{q^2 + 4p\Delta x}}{2p} \tag{8}$$

where p and q are the linear regression coefficients and the negative root $\Delta t''$ having no meaning. The small errors, in range of ±13.3 mm, were not corrected.

Laboratory tests were also carried out to fit the values of p and q and to estimate the cut-off frequencies of the different part of the system. These tests showed that the cut-off frequency of the process (hydraulic and mechanical devices), acting as a low pass filter, was above 0.3 Hz. The cut-off frequency of the signal treatment, the control and the process was evaluated at approximately 0.22 Hz.

2.3. The field experiments

The field tests were carried out just after the sowing period. The field where the test took place was 100 m long. Five tests were carried out. Each test consisted in a first passage of the drill, with the guiding assistance system turned off. On the second passage, the driver followed the usual guide (a trace left by a blade during the previous passage, Fig. 3a) while the guidance system corrected the relative position of the drill. To limit the impact of the tractor speed on the result of the tests, this speed was kept as constant as possible. In order to excite the device at higher frequencies, for two of the tests the driver was instructed to follow a sinusoidal trajectory, relative to the previous line (tests 2 and 4, with a wavelength of 20 and of 10 m, respectively). Vertical marks were placed at the nodes (at half-a-wavelength intervals), on the side of the trajectory, to help the driver (Fig. 3d). Horizontal blue marks were placed in the field of view of the camera in order to synchronise the field measurements and the data recorded by the programs (Fig. 3c, these marks did not interfere with the row detection).

Fig. 3. Presentation of the ground during the tests. (a) Guiding trace intended for the driver; (b) sowing traces (target for the camera); (c) visual horizontal marks intended for the post-treatment of the data, particularly the synchronisation of the data acquired by the computer and the ground measured data; (d) vertical marks intended for the driver for the 'sinusoidal' driving style.
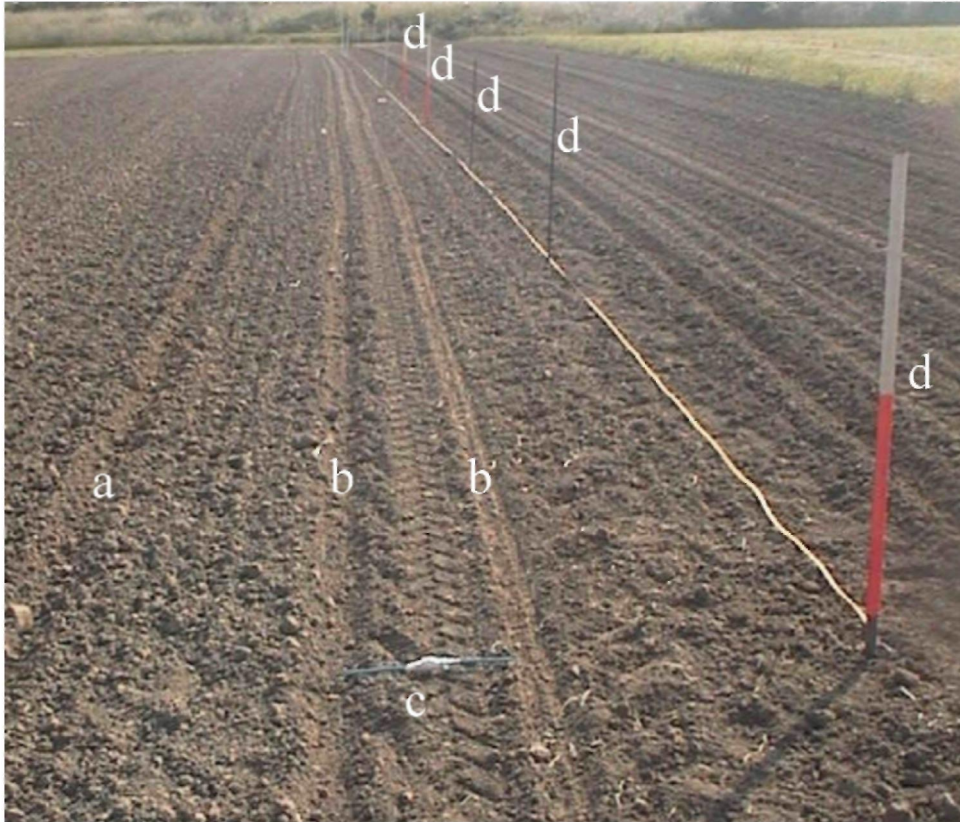
During each test, the program recorded several parameters, amongst others the time elapsed from the beginning of the test, the position x_b computed on raw data (with the Eq. (1) but using θ_m and r_m instead of $\hat{\theta}$ and $\hat{r}$), ($\hat{x}_b$) based on the estimated data ($\hat{\theta}$ and $\hat{r}$), the standard deviation sx_b of the last 20 raw positions. A video composed of the images acquired during the test and including the detected lines was also recorded. The video was used to establish the correspondence between the number of the images showing the horizontal marks at the bottom of the image, the line number in the data file and the distances in the field. This allowed the measurement noise to be determined.

After each test, the distance between the last seed line of the previous passage and the first seed line of the controlled passage were measured with a sampling interval of 0.5 m. This will be hereafter called the position of the seed drill. One of the seeding elements was lifted and a plough coulter was fixed at its place on the fixed frame attached to the tractor. The distance between the trace left by this coulter and the last seed line was also measured and was considered as the measure of the lateral displacement of the tractor (here after named position of the tractor). The beginning and the end of the line were not considered and 70 m were available for the measurements.

During the experiments, the weather was sunny. During 1 day of testing, there were some clouds and one test was carried out in diffuse lighting condition (test 5).

3. Results and discussion

The image scale was 0.37 pixels/mm at the top of the image and 1.1 pixels/mm at the bottom. The tractor speed varied from 0.91 to 0.95 m/s. The image acquisition frequency varied from 9.9 to 10.2 images per second when a video was recorded (otherwise, the 15 images per second delivered by the camera can be processed). These data were considered to be sufficiently constant to have no effect on the behaviour of the control.

The distances measured in the field after the tests are presented first and the data recorded by the computer during the test will be analysed next. The main results are summarised in Table 1. The field measurements are presented in detail under different graphical forms for the two first tests: Figs. 4 and 5 plot the position of the tractor and of the seed drill against the covered distance; Figs. 6 and 7 show the histograms of the positions while Figs. 8 and 9 show the amplitudes of the frequency decomposition of the tractor and of the drill positions. For a better readability of the graphs in Figs. 4-7 the data were centred. A detrend process was applied to the data before the Fourier transform in Figs. 8 and 9.

During the first test, the instruction to the driver (who was not a trained driver) was to follow the previous lines.

It is obvious that the observed trajectory was not parallel to the previous one but deviated and that the driver corrected twice at around 20 m and at around 40 m (it is not possible to know from these data whether these deviations were made during the first passage, during the second one or during both). However, apart from these corrections, the trajectory was rather straight. The aim of the sinusoidal driving style as in the second test, was to provide external disturbances of higher frequencies. Even if this was not as obvious in Fig. 4, the shift of the frequency having the maximum amplitude was observed in Fig. 9 (0.04 m^{-1}) compared with Fig. 8 (0.03 m^{-1}).

The mean position of the seed drill (trueness m_D, Table 1) depends on the mounting of the camera. For the first two experiments, this was done carefully and the values were close to the theoretical width of 450 mm. For the other tests, the mounting was done more approximately (because it required time) and the values were less precise. This, however, does not seems to be a real problem for the eventual industrial application. There was another origin for a difference between the target value (450 mm) and the measurements. The border of the trace left by the drill was sometimes more visible than the central hollow, as can be observed in Fig. 1. In this case, the mean position can deviate by 20-30 mm.

Table 1. *Main results of the five field tests*

Test	Driving style	S_T	r_T	m_D	S_D	r_D	sx_b	rx_b	msx_b
1	'Straight'	75.1	295	459	19.4	91	9.2	41	7.6
2	'Sinusoidal', wavelength 20 m	102	340	448	29	115	18.7	46	12.1
3	'Straight'	81	245	523	13	60	8.5	34	8.6
4	'Sinusoidal', wavelength 10 m	55	301	516	35	140	18.6	64	10.7
5	'Straight'	54	180	390	17	95	12.8	51	10

S_T is the standard deviation of the tractor's position; r_T is the range of the tractor's position; m_D is the drill's mean position; s_D is the standard deviation of the drill's position; r_D is the range of the drill's position; sx_b is the standard deviation of the estimated position $\hat{x}_b$ (computed for the whole test); rx_b is the range of the estimated position $\hat{x}_b$; msx_b is the mean on a whole test of standard deviation of last 20 raw positions. All the data are given in mm.

Though the reduction in the ranges of the movements of the drill (the response) compared with the range of the tractor's movements (the disturbance) can be seen in Figs. 4 and 5, it can be better evaluated in Figs. 6 and 7, as well as in Table 1. The dispersion of the drill's position was symmetrical around the mean and appeared bell-shaped (especially in Fig. 6) while the distribution of the tractor's position was more flat. This change in the shape of the distribution is corroborated by the data: the standard deviation of the positions dropped from 73 mm for the tractor (mean value of S_T, Table 1) to 23 mm for the drill (mean of s_D-that is a ratio of 3.17) while the corresponding value for the ranges lessened from 272 to 100 mm (respectively, means of A_T and A_b-ratio of 2.72). As the harvesting machines, which would eventually harvest the crop can tolerate up to 150 mm misalignments between row sown by different passages, the values of the trueness, of the precision and of the range are well within this tolerance and are thus totally compatible with this application. For applications such as mechanical weeding, better performances should, however, be achieved. Tests 1, 3 and 5, for which the driver was instructed to drive "straight", showed lower values of dispersion of the drill's position than tests 2 and 4 for which the driving was of sinusoidal type (standard deviation and range below the corresponding means for the first group, above for the second). The lighting conditions were not found to have any effect neither on the trueness, nor on the precision.

Fig. 4. *Position of the tractor and of the seed drill relative to the previous seed row, against the covered distance. Test 1, centred data. In grey: the position of the tractor; in black: the position of the actual seed row.*
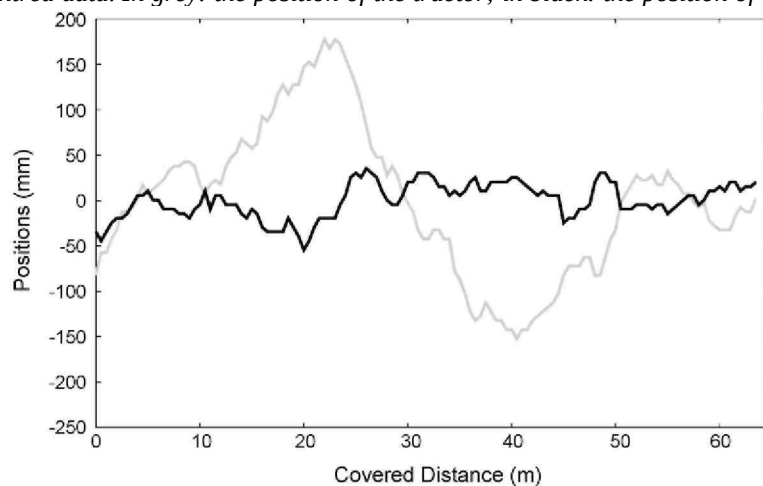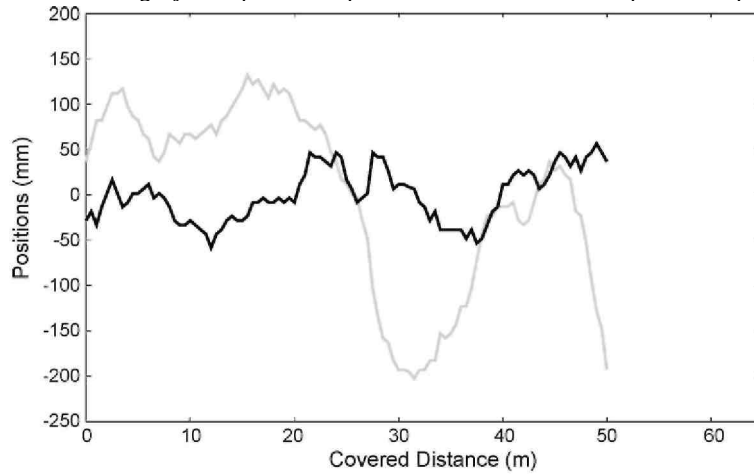
Fig. 5. *Position of the tractor and of the seed drill relative to the previous seed row, against the covered distance. Test 2, centred data. In grey: the position of the tractor; in black: the position of the actual seed row.*

Fig. 6. *Histograms of the position of the tractor and of the seed drill relative to the previous seed row. Test 1, centred data. In grey: the position of the tractor; in black: the position of the actual seed row.*
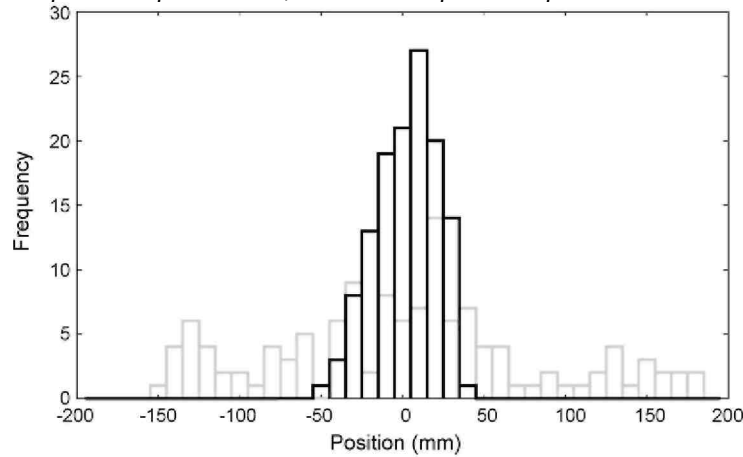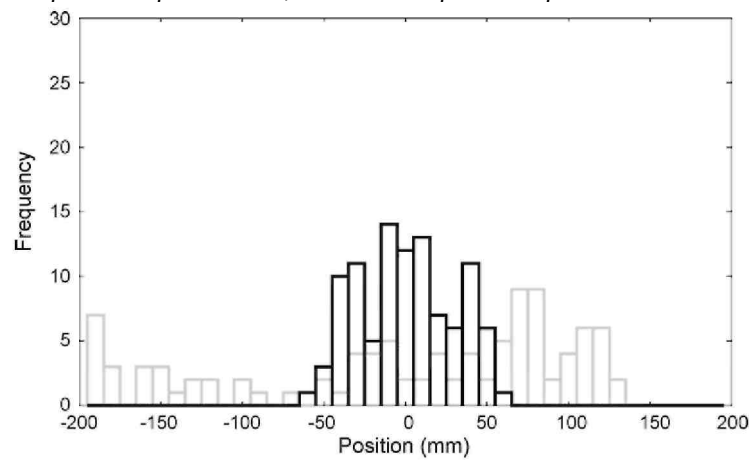

Fig. 7. *Histograms of the position of the tractor and of the seed drill relative to the previous seed row. Test 2, centred data. In grey: the position of the tractor; in black: the position of the actual seed row.*

Fig. 8. *Frequency analysis of the movements of the tractor and of the seed drill, Test 1. In greys, amplitudes of the tractor displacements; in black, amplitudes of the seed drill displacements.*
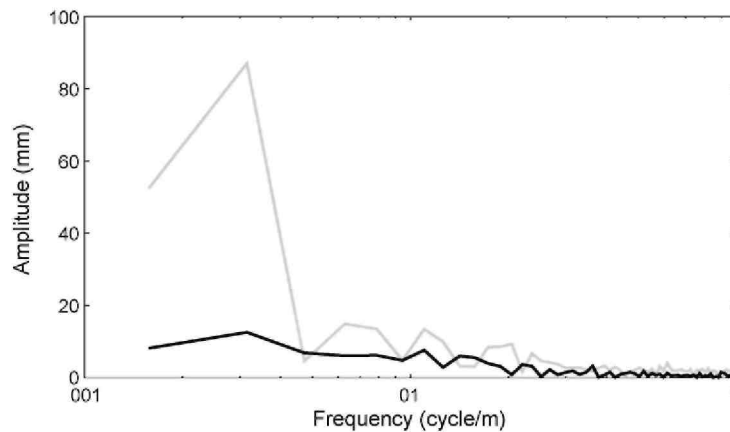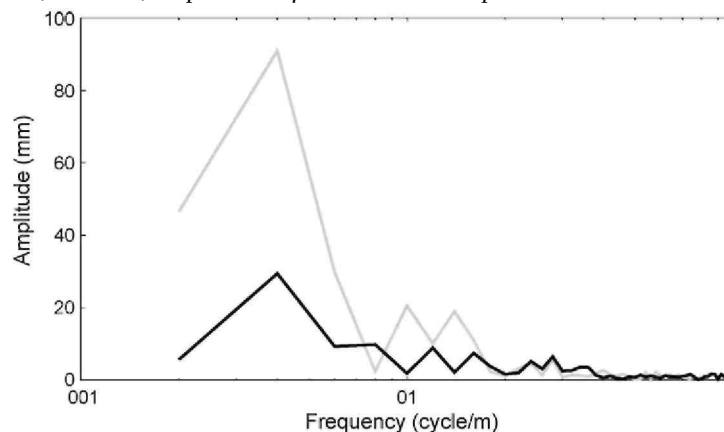
Fig. 9. *Frequency analysis of the movements of the tractor and of the seed drill, Test 2. In grey, amplitudes of the tractor displacements; in black, amplitudes of the seed drill displacements.*

The causes of dispersion of the position of the drill was linked to the lack of ability of the system to correct the movements of the tractor (the process noise) and to lack of ability to remove the measurement noise during the signal treatment, or to the delay in doing such corrections. The signal treatment (Fig. 2) acts as a low-pass filter. Its output was subtracted from the target position and transformed into pulse width by the regulator. When the result of the process was added to the previous position, the low frequencies of the process noise, only slightly attenuated by the signal treatment, disappeared from the next position while higher frequencies, which were more attenuated, remained in the output. On the other hand, the noise added during the measurement was filtered in the same way. Its low frequency content was not removed by the signal treatment and was also found in the correction. The following discussion tend to make the part between those two error sources.

As noted in Section 2.2.3, the cut-off frequency of the mechanical and hydraulic part was approximately 0.3 Hz (taking into account the speed of the tractor, the corresponding spatial frequency should have been slightly above 0.3 cycle/m). The diagrams in Figs. 8 and 9 show that at and above 0.3 Hz, the tractor movements were quite small and the mechanical filtering fortunately did not play a significant role in the control. The same diagrams show that the amplitudes of the drill movements were quite smaller than those of the tractor's movements, especially for the low frequencies. In order to facilitate the determination of the cut-off frequency of the control in field conditions, the ratio of the amplitudes of the tractor's movements to the amplitude of the seed drill's movement was computed. This ratio was smoothed by computing the mean ratio of the five tests. The cut-off frequency, evaluated as the frequency showing an amplitude ratio of -3dB, was of 0.14 cycle/m, corresponding to a wavelength of 7 m. This spatial frequency was slightly lower than the evaluation made in the laboratory. The values of Δt, computed using Eq. (8), recorded by the control program during the field test were compared to the measurements of Δx in the field. It was concluded that the value of υ was lower in the field conditions and that the parameter p (Eqs. (5)-(8), estimated in the laboratory) was slightly over-estimated, which could partly explain a slower reaction. The two sinusoidal tests had wavelengths of 20 and 10 m and their estimated peak amplitudes ratio were, respectively, -9.75 dB (0.33) and -5.5 dB (0.53), indicating that a significant part of their process noise remained at the output of the control. However, observing Fig. 8, it must be noticed that with a "normal" driving style, the amplitudes at these wavelengths were already low. This corroborates the observations made from Table 1: when the driver adopted a 'soft' driving style, the control was able to operate more accurately

than in the case of rapid direction changes.

The measurement noise was analysed using both field measurements, recorded data and the videos. Differences may be observed between the standard deviations and the ranges of different measures in Table 1. The standard deviation of the displacement of the trace measured in the image (i.e. the displacement of the seed drill relatively to the previous rows, as seen from the seed drill) $s(\hat{x}_b)$ was systematically lesser than the standard deviation of the traces of the seed drill relatively to the previous traces (i.e. the measures on the ground; S_b)· The corresponding ranges were also usually much smaller. These differences have to be explained. The noise resulting from the images analysis was conform to the previous studies (Leemans and Destain, 2006) showing similar values of precision (22 mm, before filtering). Its low frequency content had low amplitudes, with peak amplitudes around 5-8 mm (unshown) and its contribution to S_b was relatively small, compared to the amplitude of 30 mm for the drill, in Fig. 9. Beside the measurement noise other errors in the estimation of the position were observed. Two geometrical systematic errors were identified. The first one was linked to the angle of the tool relative to the previous line (Θ, in the field plane). The position was estimated at the bottom of the image but the traces left by the seeding element were made 1.5 m behind the image (as it can be seen Fig. 7, above). When the trajectory of the tractor was not parallel to the previous row, the position of the seeding element was then misestimated by (in mm):

$$1500 \times tg(\Theta).$$

The correction of this error could be quite straight-forward though the angle must be estimated correctly, which requires a correct alignment of the camera. A misaligment of 0.015 rad. (0.85°) would thus produce an error in the range of the standard deviation of the position. Tillett et al. (2002) overcame this problem by adding it as a third state variable (with the lateral position and the angle). Another source of error came from the difference of curvature between the previous row and the actual trajectory. This would be more complex to deal with, as the curvature could not be evaluated within an image, the portion of rows observed being too short. The difference in curvature should be inferred from the changes in the angle between previous and actual values of Θ or from the steering angle of the tractor's steering wheels. As explained above, an accurate evaluation of this angle could be used to enhance the prediction of $\hat{r}$ and increase the cut-off frequency. Because of their origin, these two errors are linked to the state variables $\hat{r}$ and $\hat{\theta}$ and have a similar spectral distributions. They could thus not be eliminated by filtering. On an other hand, they could be reduced by moving the field of view back to near the sowing element. This requires either tilting the camera or moving it backwards.

The standard deviation sx_b of the last 20 raw positions (whose mean value msx_b is given in Table 1) was found only roughly correlated with either the measurement noises or the noise resulting from the image analysis. This parameter could thus not be used as a warning for a drop of reliability or of performance of the regulation.

4. Conclusions

The performances of a guidance assistance mechanism and control algorithm, dedicated to sugarbeet precision seed drill, was analysed during field tests. The data of the control program were recorded and the difference between the observed inter-row distance and its nominal value (450 mm) were measured on the ground.

It was found that the trueness of the system (the mean of the difference between the measurement and the set value) was strongly influenced by the mounting of the camera. When this camera was mounted properly, the trueness was below 30 mm, due mainly to the aspect of the trace left by the drill. The precision (the standard deviation of the above difference) was of 23 mm and the range of 100 mm, while the corresponding values for the tractor were of 73 and 272 mm, respectively. These values would ensure the compatibility of seed drill equipped with a guidance assistance with a non-matching width harvesting machine. During the field tests, the driver was asked to drive normally for some tests and to drive sinusoidally for the others. The value of precision and range of the former driving style were lower than those of the latter. This means that rapid direction changes should be avoided, in favour of a smoother driving style.

A detailed analysis of the results showed that the whole system acted as a low pass filter having a cut-off spatial frequency of 0.14 m^{-1}. Apart from the measurement noise, two other errors sources were identified. The first one was linked to the distance between the estimated position of the drill (at the bottom of the image) and the actual position and the second to the difference of curvature between the previous row and the actual trajectory. The correction of the first error as well as the increase of the cut-off frequency could be achieved by better taking into account the orientation of trace in the image. This requires accurate mounting of the camera, which was not possible in the context of these experiments, but could be achieved for an industrial application.

Acknowledgements

References

Billingsley, J., Schoenfisch, M., 1997. The successful development of a vision guidance system for agriculture. Comput. Electron. Agric. 16, 147-163.

Hague, T., Marchant, J.A., Tillett, N.D., 2000. Ground based sensing systems for autonomous agricultural vehicles. Comput. Electron. Agric. 25, 11-18.

Leemans, V., Destain, M.-F, 2006. First step to seed drill guidance assistance by using machine vision. Biosyst. Eng. 94 (3), 325-336.

Pilarski, T., Happold, M., Pangels, H., Ollis, M., Fitzpatrick, K., Stentz, A., 2002. The Demeter system for automated harvesting. Auton. Robot. 13, 9-20.

Søgaard, H.T., Olsen, H.J., 2003. Determination of crop rows by image analysis without segmentation. Comput. Electron. Agric. 38, 141-158.

Tillett, N.D., Hague, T., 1999. Computer-vision based hoe guidance for cereals-an initial trial. J. Agric. Eng. Res. 74, 225-236.

Tillett, N.D., Hague, T., Miles, S.J., 2002. Inter-row vision guidance for mechanical weed control in sugar beet. Comput. Electron. Agric. 33, 163-177.